The advanced evolutionary phases of the massive stars and their explosive yields

JINA workshop on Massive Stellar Progenitors: "The Final Days of Burning"
March 9-10, 2006, Santa Barbara

Alessandro Chieffi

Istituto Nazionale di AstroFisica (Istituto di Astrofisica Spaziale e Fisica Cosmica)

&

Centre for Stellar and Planetary Astrophysics – Monash University - Australia

Email: alessandro.chieffi@iasf-roma.inaf.it

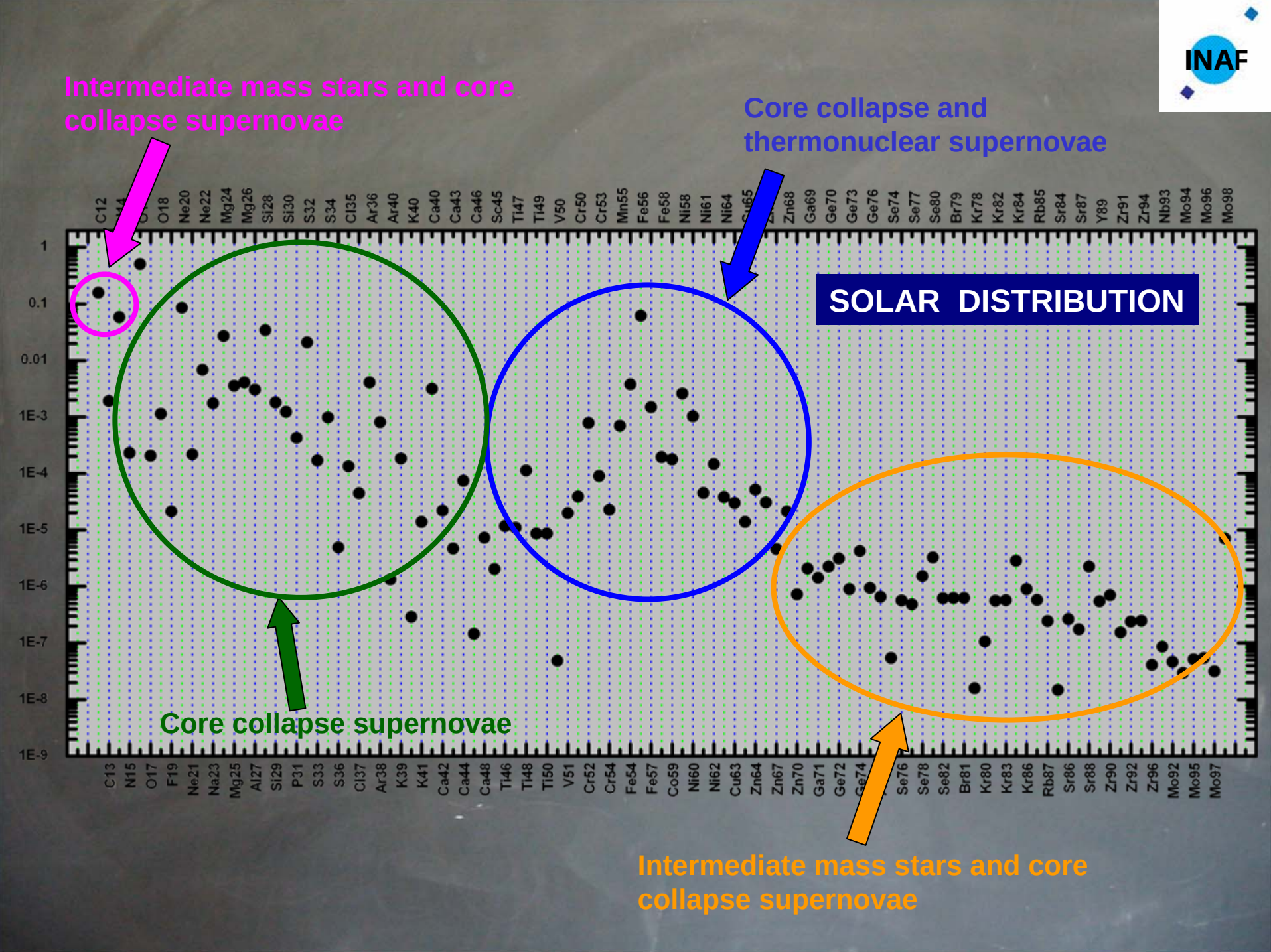
Intermediate mass stars and core collapse supernovae
Core collapse and thermonuclear supernovae
SOLAR DISTRIBUTION
Core collapse supernovae
Intermediate mass stars and core collapse supernovae
INAF

BASIC PROPERTIES OF THE SHOCK WAVE:

RADIATION DOMINATED: $\Rightarrow$ $E = \frac{4}{3}\pi a r^3 T^4$

ADIABATIC EXPANSION: $\Rightarrow$ $T = const \cdot r^{\frac{3}{4}}$

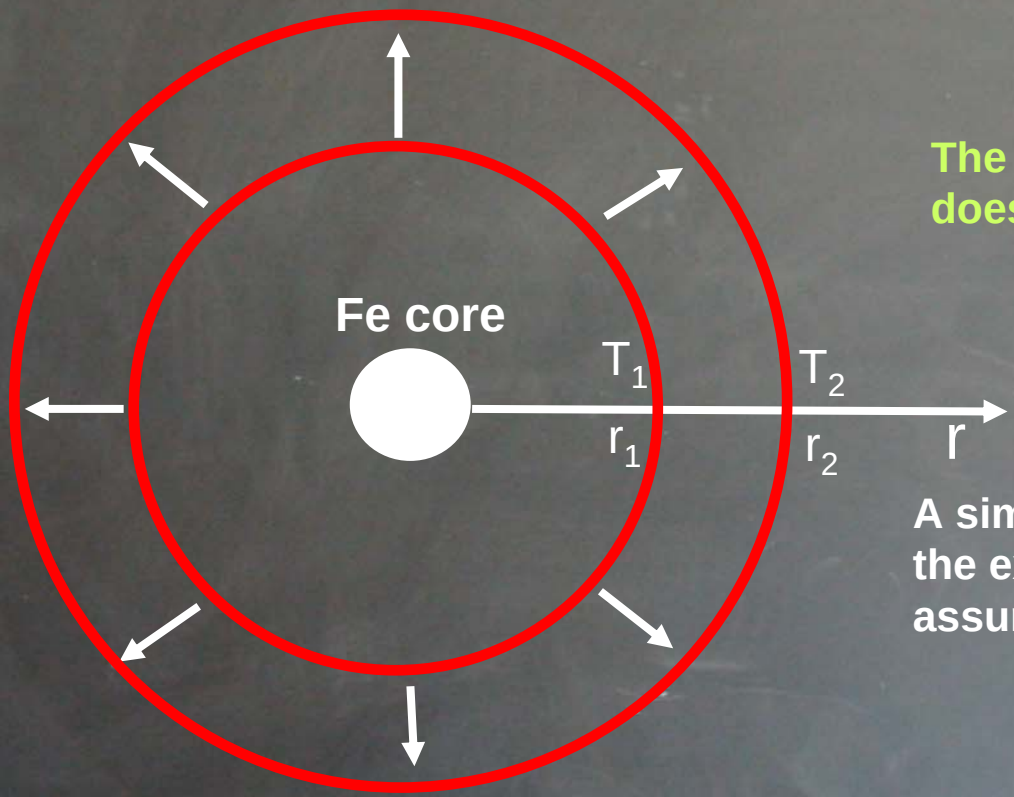

CONSEQUENCE:

The peak temperature of the blast wave does not depend on the stellar structure

A simple but quite effective computation of the explosive yields may be obtained by assuming:

$$T(t) = T_{peak} e^{-\frac{t}{\tau}}$$

$$\tau = (\alpha 24\pi G)^{-.5} \rho_{peak}^{-.5}$$

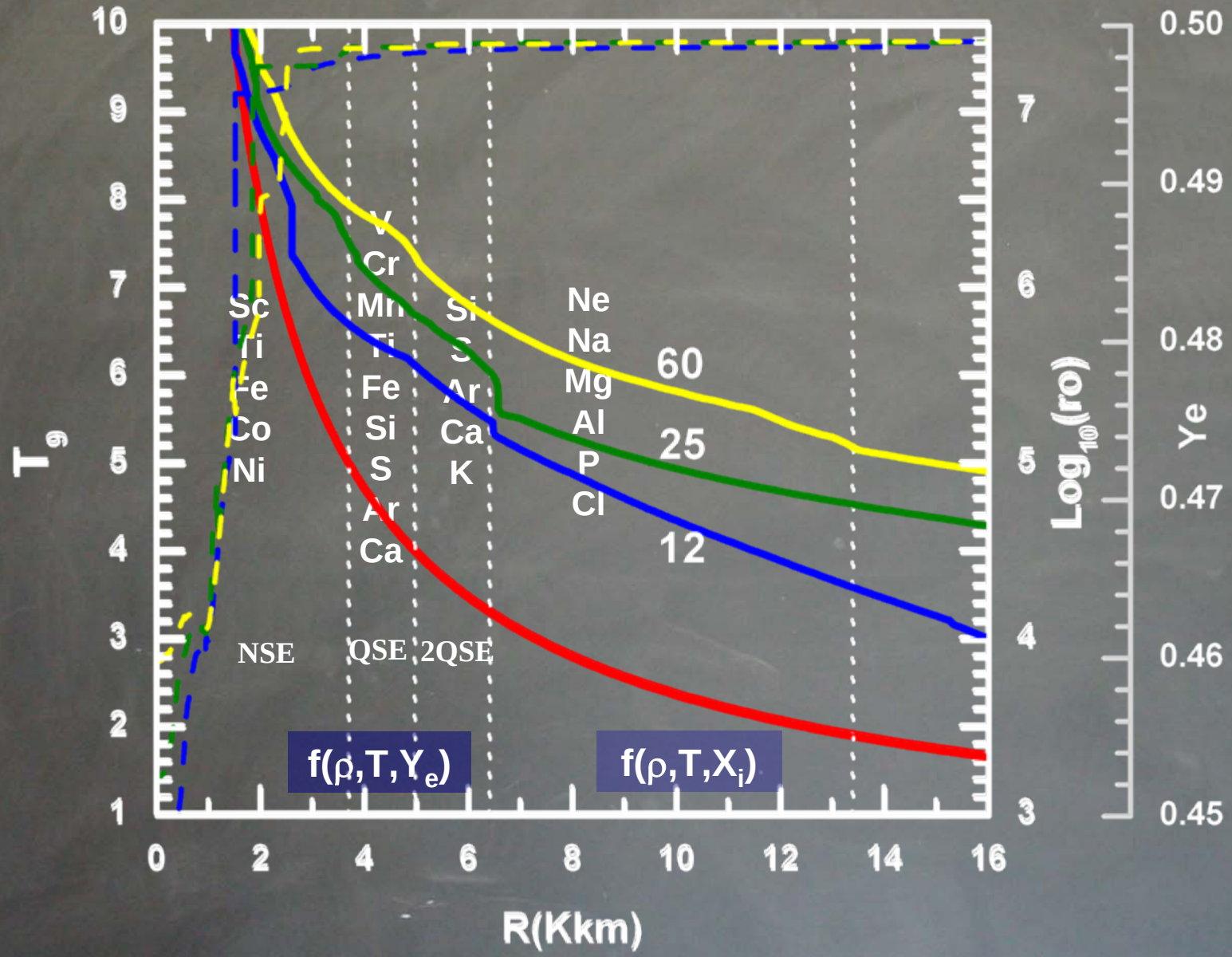
INAF
T_9
$Log_{10}(\rho)$
Ye
R(Kkm)
Sc
Ti
Fe
Co
Ni
V
Cr
Mn
Ti
Fe
Si
S
Ar
Ca
Si
S
Ar
Ca
K
Ne
Na
Mg
Al
P
Cl
60
25
12
NSE
QSE
2QSE
$f(\rho,T,Y_e)$
$f(\rho,T,X_i)$

H burning

Monoparametric sequence of models

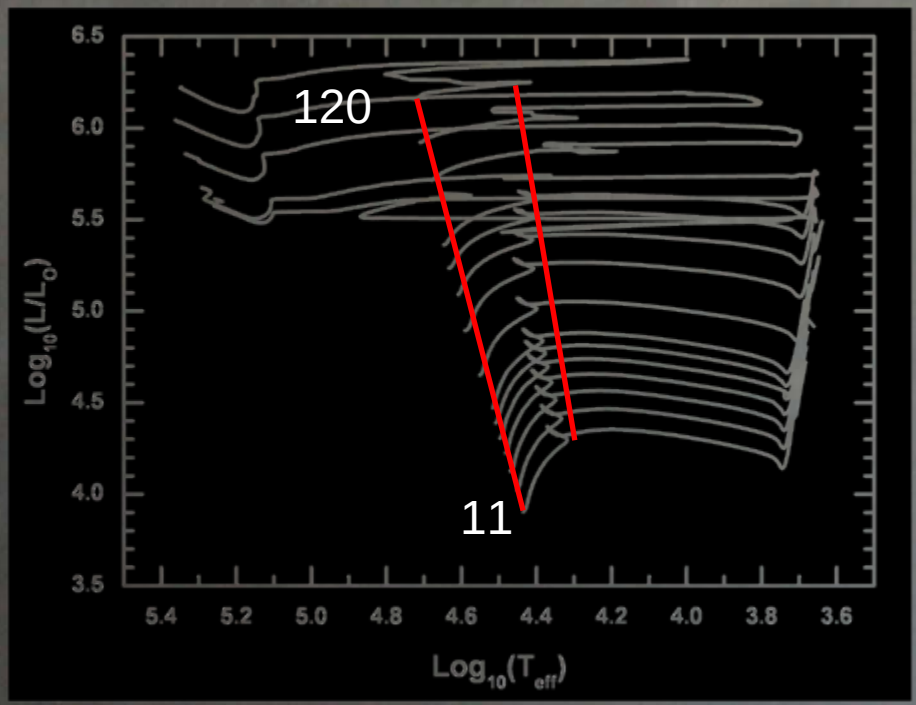

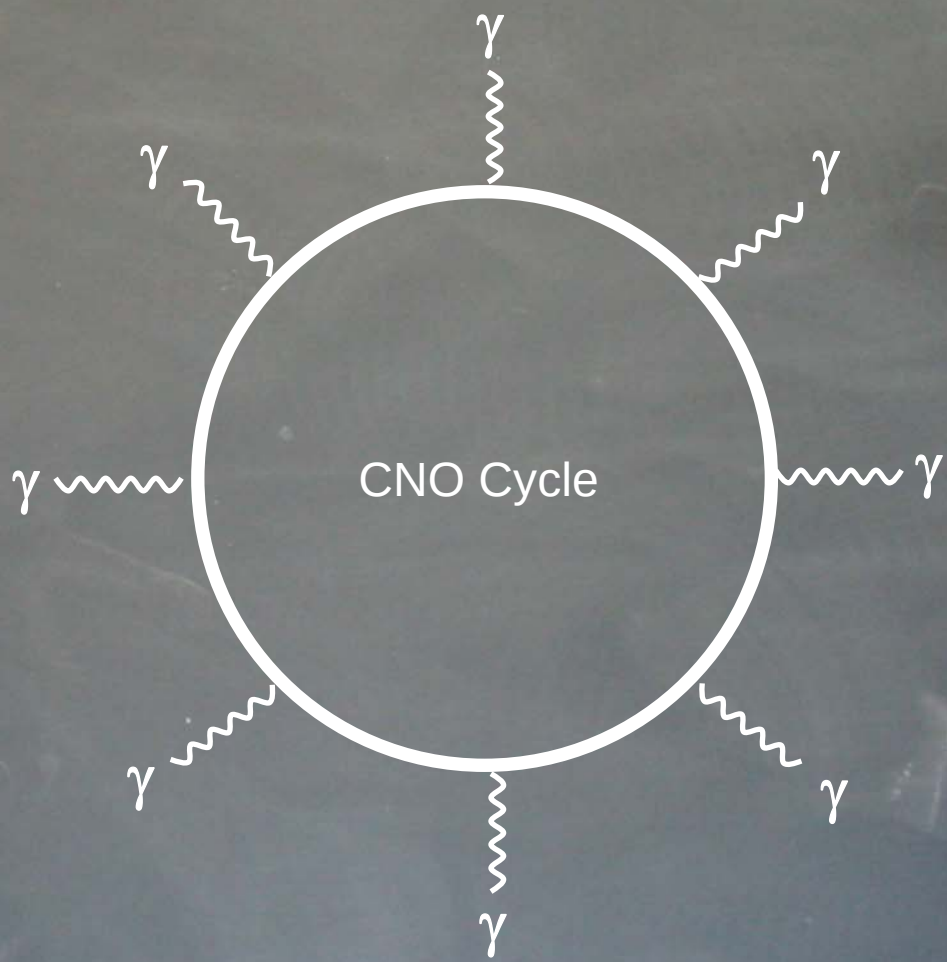

He burning

Monoparametric sequence of models

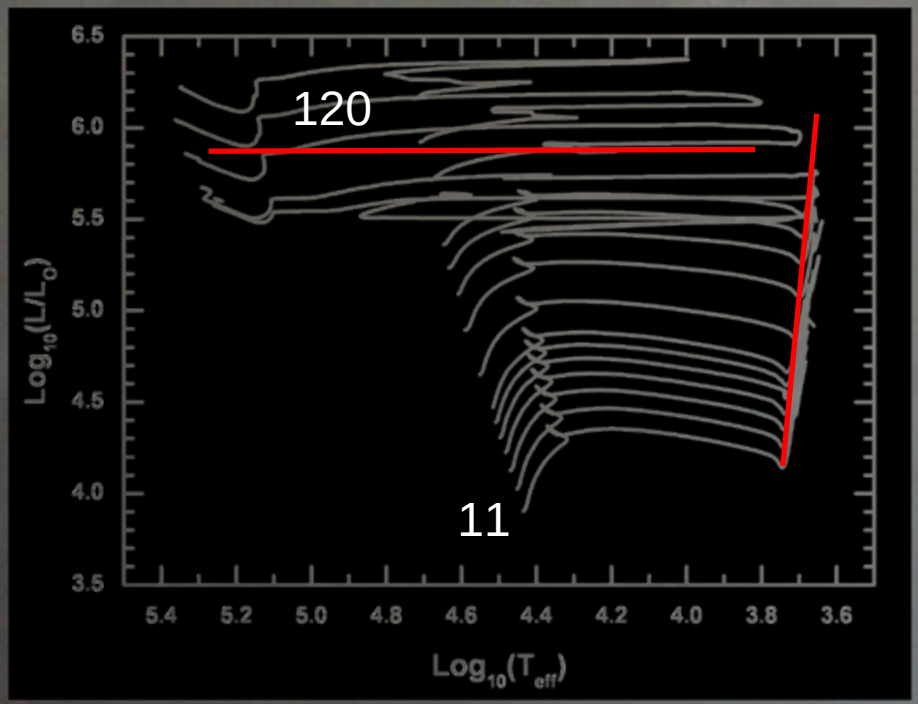

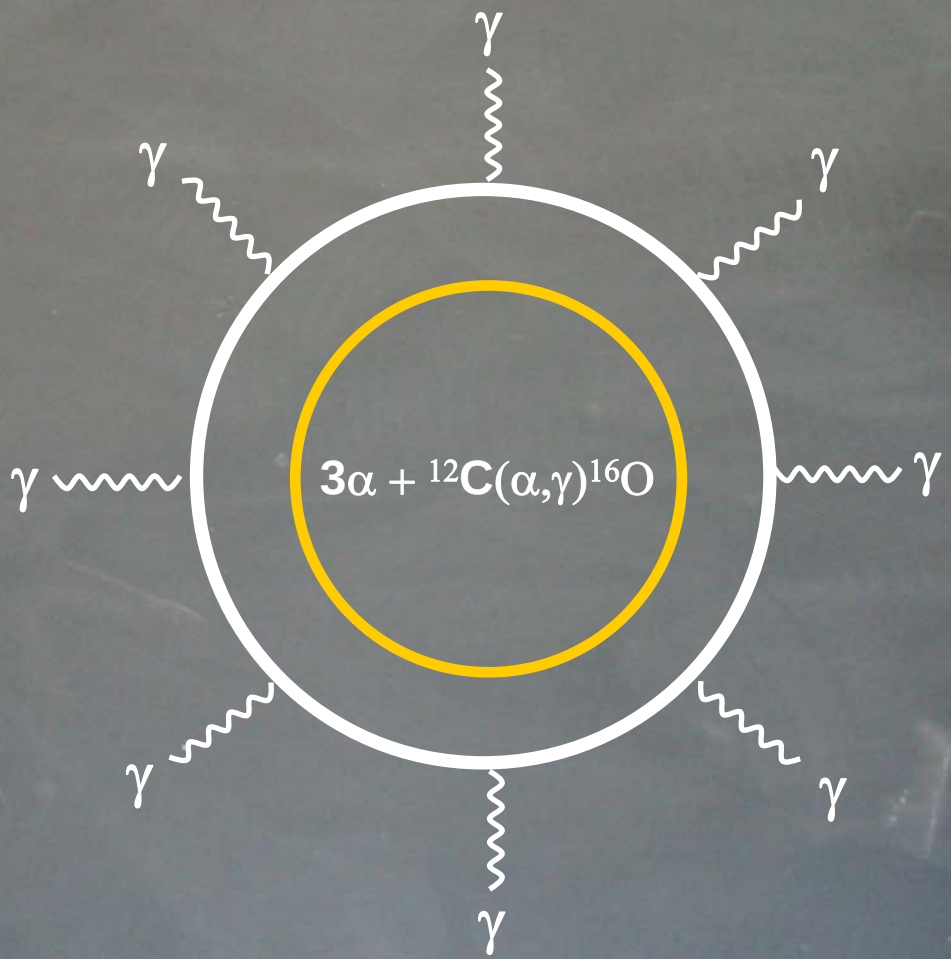

C burning

NOT a monoparametric sequence of models any more

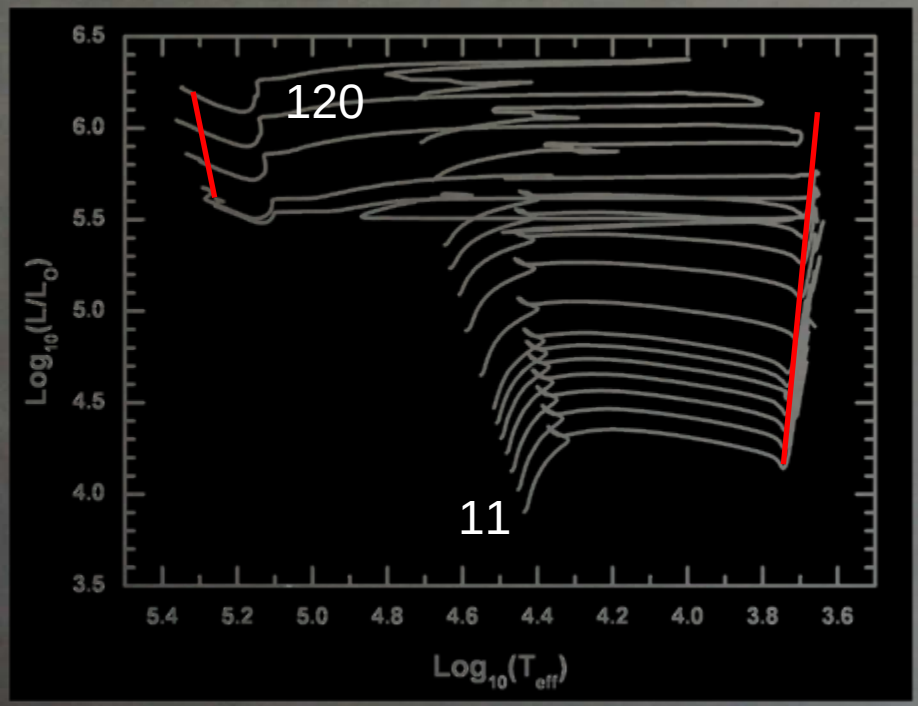

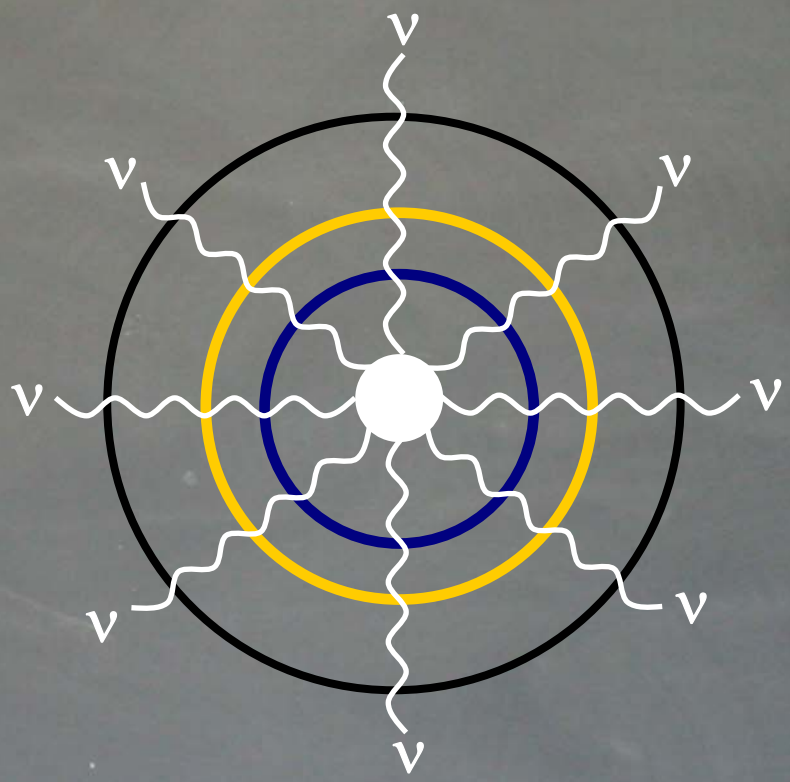

^{12}C (^{12}C , p) ^{23}Na (p , α) ^{20}Ne

^{12}C (^{12}C , α) ^{20}Ne

^{16}O (α , γ) ^{20}Ne

C burning

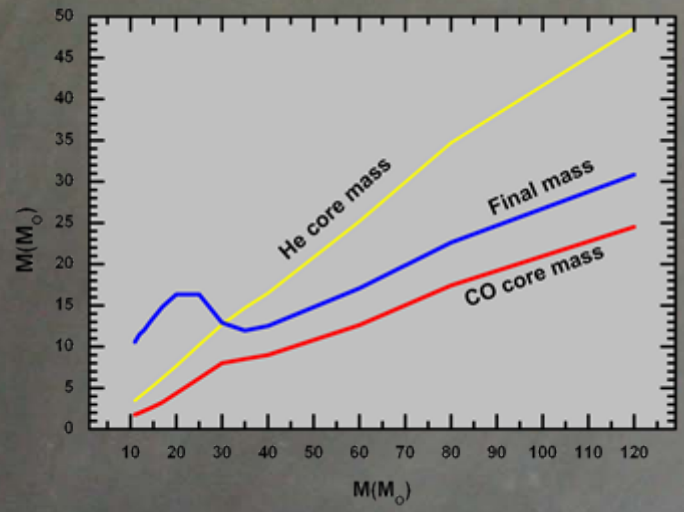
He core mass
Final mass
CO core mass
M(M$_O$)
M(M$_O$)

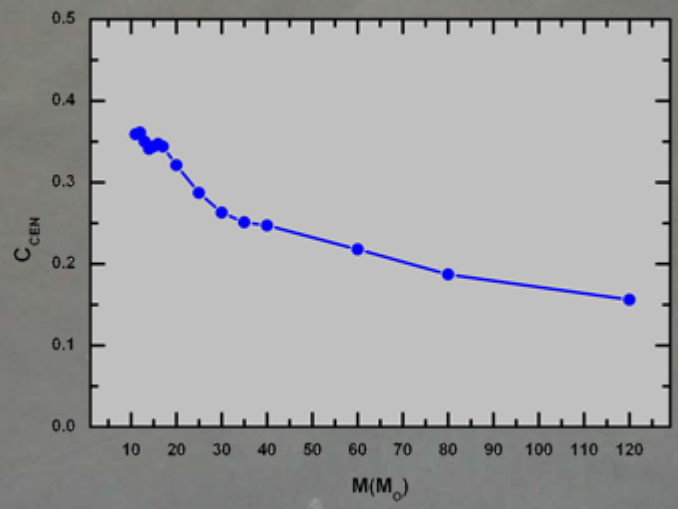
C$_{CEN}$
M(M$_O$)

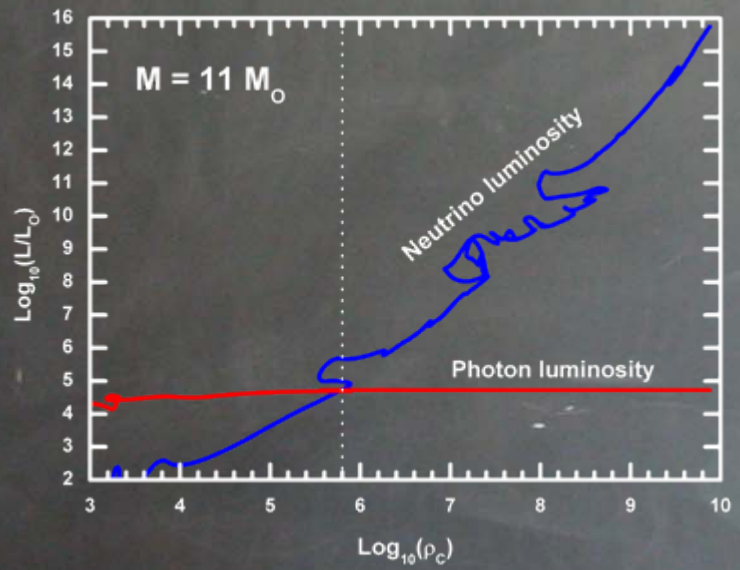
M = 11 M$_O$
Neutrino luminosity
Photon luminosity
Log$_{10}$(L/L$_O$)
Log$_{10}$(ρ$_C$)

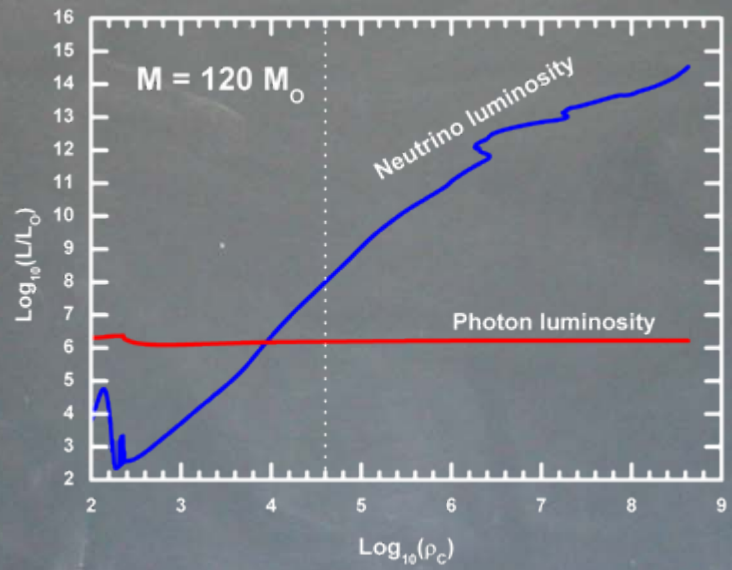
M = 120 M$_O$
Neutrino luminosity
Photon luminosity
Log$_{10}$(L/L$_O$)
Log$_{10}$(ρ$_C$)

C burning

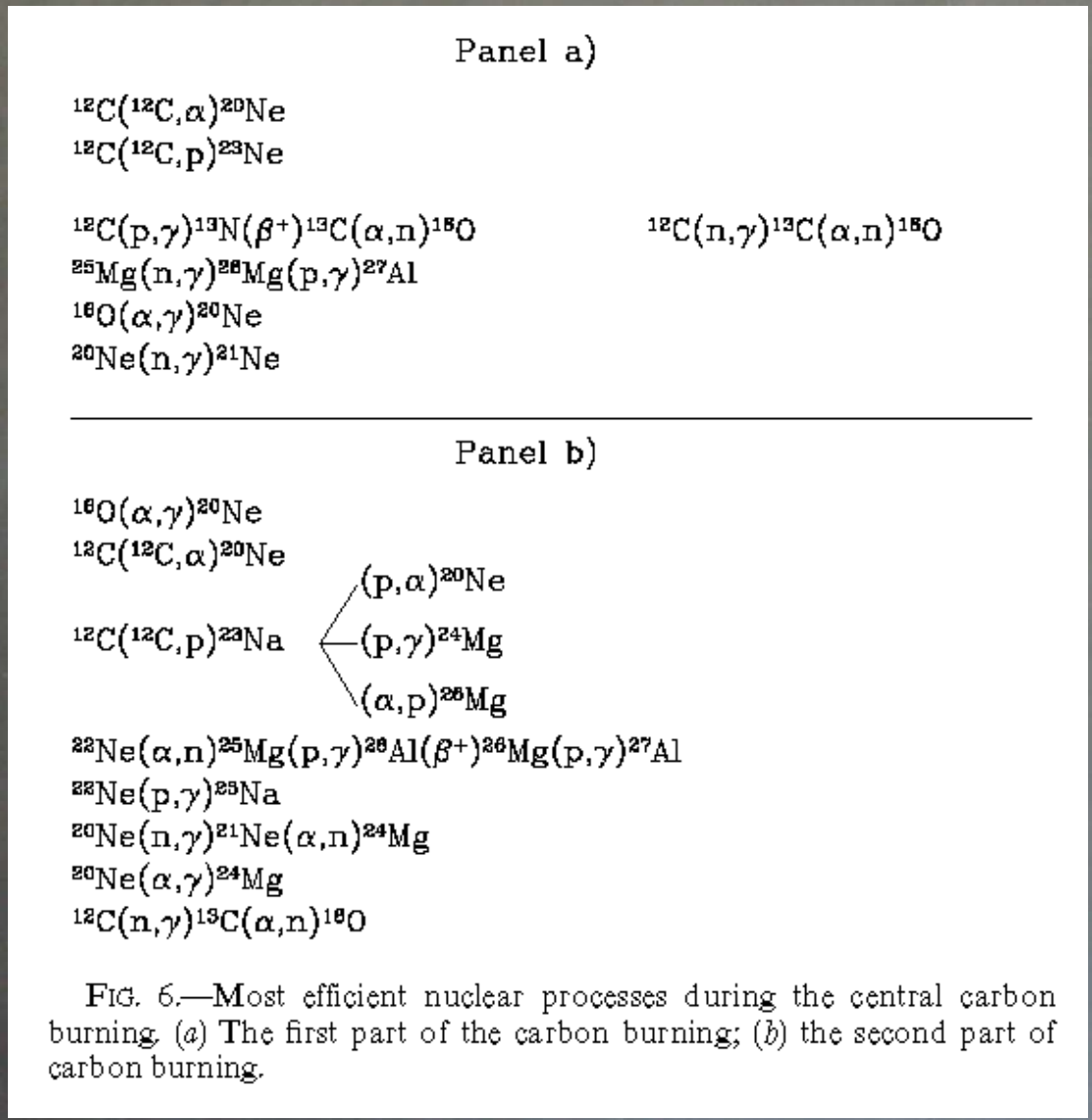

FIG. 6.—Most efficient nuclear processes during the central carbon burning. (*a*) The first part of the carbon burning; (*b*) the second part of carbon burning.

Ne burning

NOT a monoparametric sequence of models

$^{20}Ne\ (\gamma\ ,\alpha)\ ^{16}O$

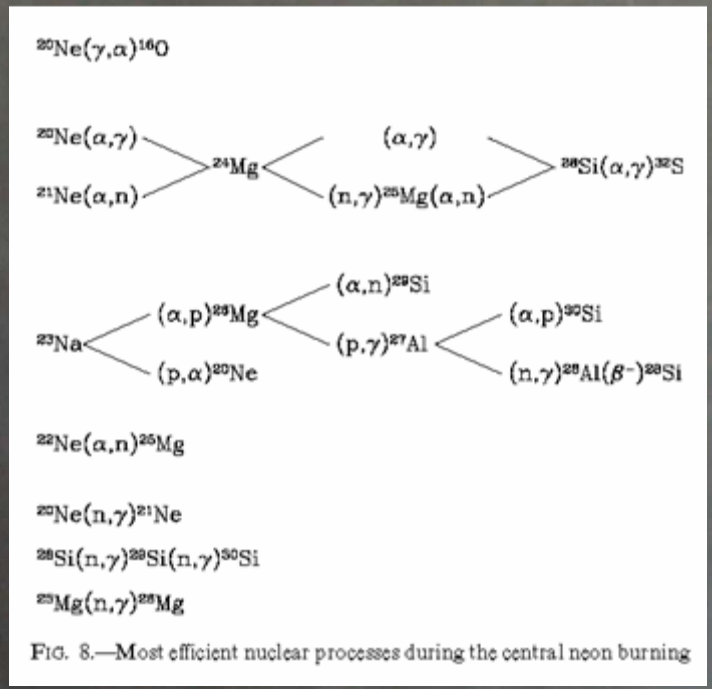

FIG. 8.—Most efficient nuclear processes during the central neon burning

O burning

$^{16}O\ (\ ^{16}O\ ,\ p\ )\ ^{31}P(\ p\ ,\ \alpha\ )\ ^{28}Si\ (\ \alpha\ ,\ \gamma\ )\ ^{32}S$

$^{16}O\ (\ ^{16}O\ ,\ \alpha\ )\ ^{28}Si$

$^{16}O\ (\ ^{16}O\ ,\ n\ )\ ^{31}S(\ \beta^+\ )\ ^{31}P$

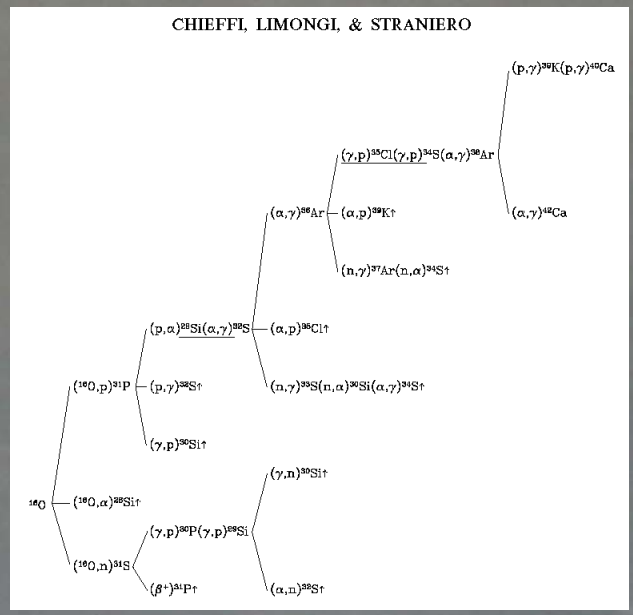

TABLE 7

INTEGRATED FLUX OF THE MOST EFFICIENT WEAK INTERACTIONS DURING CENTRAL O BURNING FOR 15 $M_\odot$ AND 25 $M_\odot$

Reaction	15 $M_\odot$	25 $M_\odot$
$^{31}S(\beta^+)^{31}P$	6.7(19)	6.4(16)
$^{33}S(e^-, \nu)^{33}P$	1.2(19)	3.0(15)
$^{30}P(e^-, \nu)^{30}Si$	3.7(18)	9.8(14)
$^{37}Ar(e^-, \nu)^{37}Cl$	3.1(18)	2.8(15)
Maximum integrated flux	5.4(21)	9.9(19)
Y_e	0.488	0.495

Beyond O burning

a (b , c) d ⇄ d (c , b) a

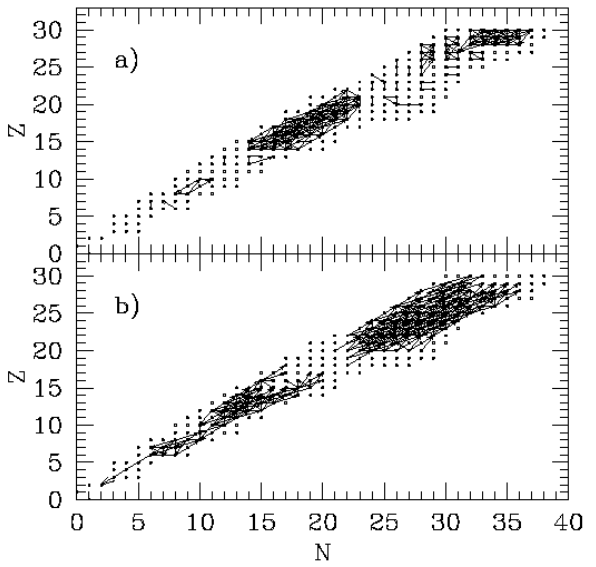

FIG. 14.—Effective processes in the (N, Z)-plane having (a) $\varphi < 0.1$ and (b) $\varphi > 0.1$ in the phase extending between the central oxygen exhaustion and the central silicon ignition (see text).

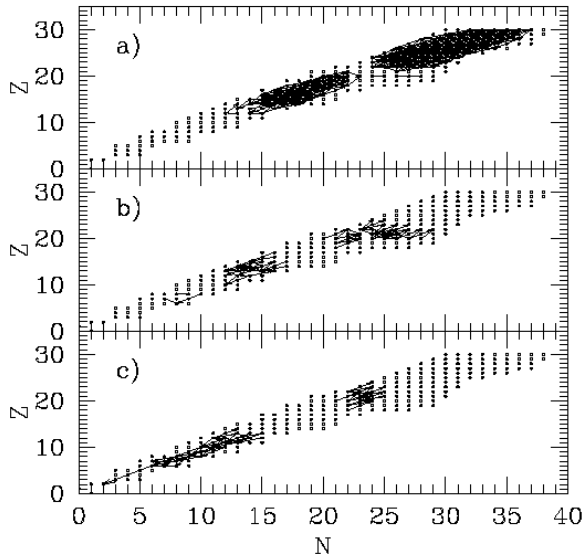

FIG. 16.—Effective processes in the (N, Z)-plane having (a) $\varphi \leq 0.01$, (b) $0.01 < \varphi \leq 0.1$, and (c) $\varphi > 0.1$ just after the formation of the silicon convective core, i.e., when the central temperature is 3.5×10^9 K.

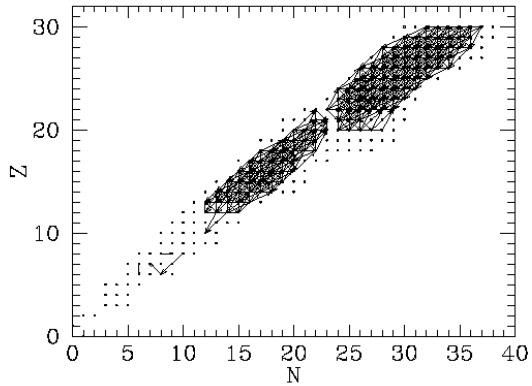

FIG. 17.—Composite plot of the effective processes shown separately in the two panels of Fig. 16.

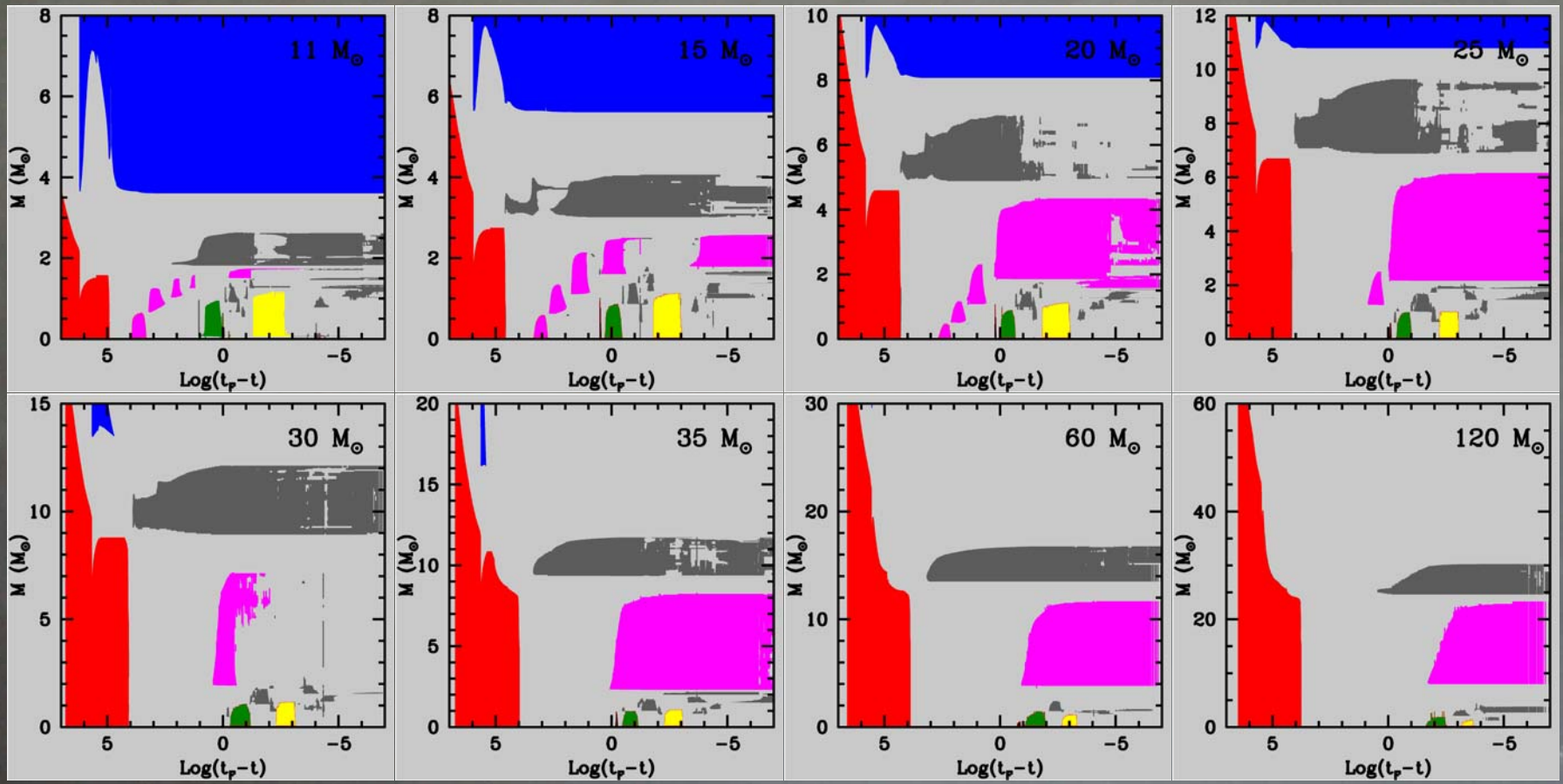
11 M⊙
15 M⊙
20 M⊙
25 M⊙
30 M⊙
35 M⊙
60 M⊙
120 M⊙
M (M⊙)
Log(tP−t)

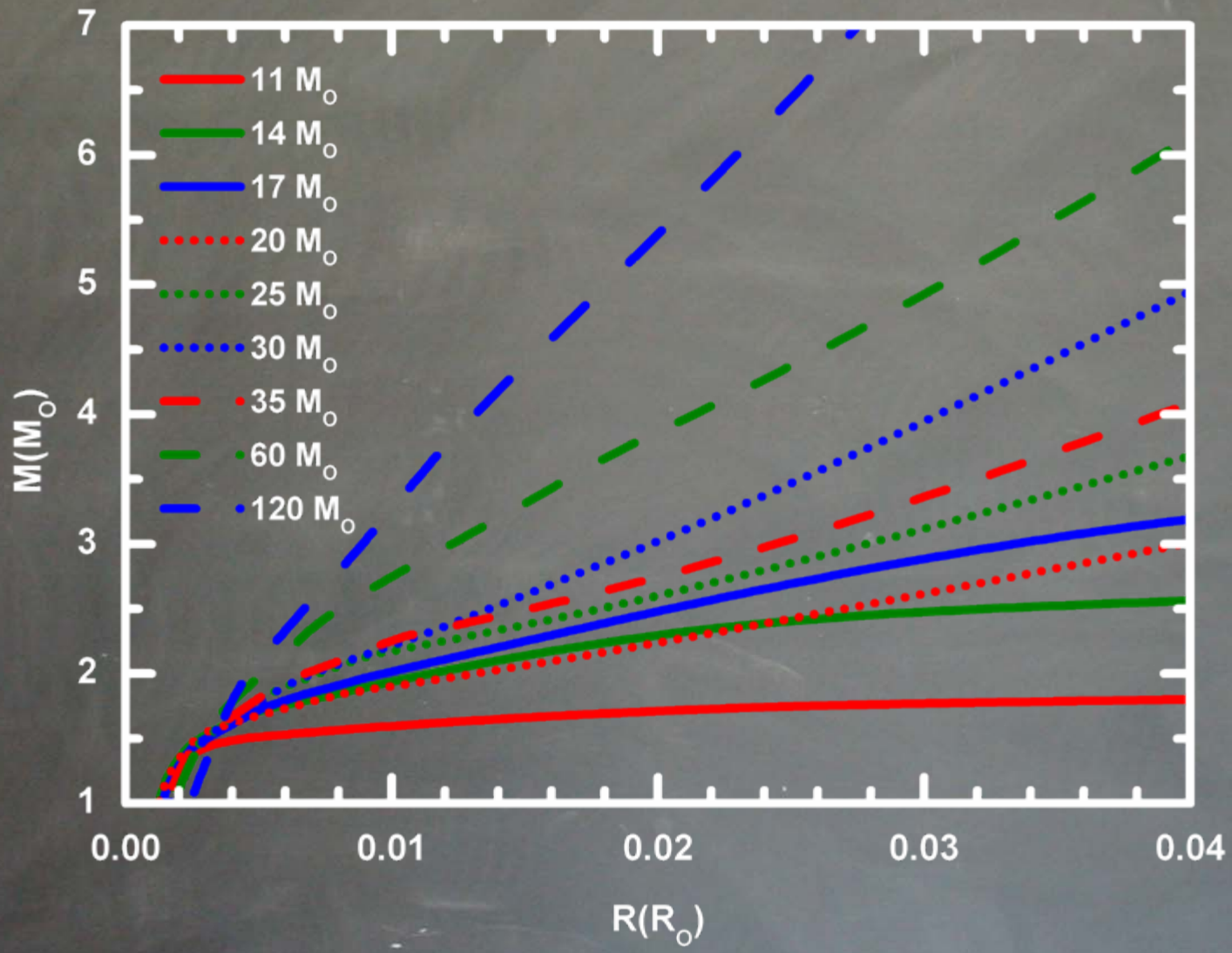
11 M$_O$
14 M$_O$
17 M$_O$
20 M$_O$
25 M$_O$
30 M$_O$
35 M$_O$
60 M$_O$
120 M$_O$
M(M$_O$)
R(R$_O$)
7
6
5
4
3
2
1
0.00
0.01
0.02
0.03
0.04

11 M_O

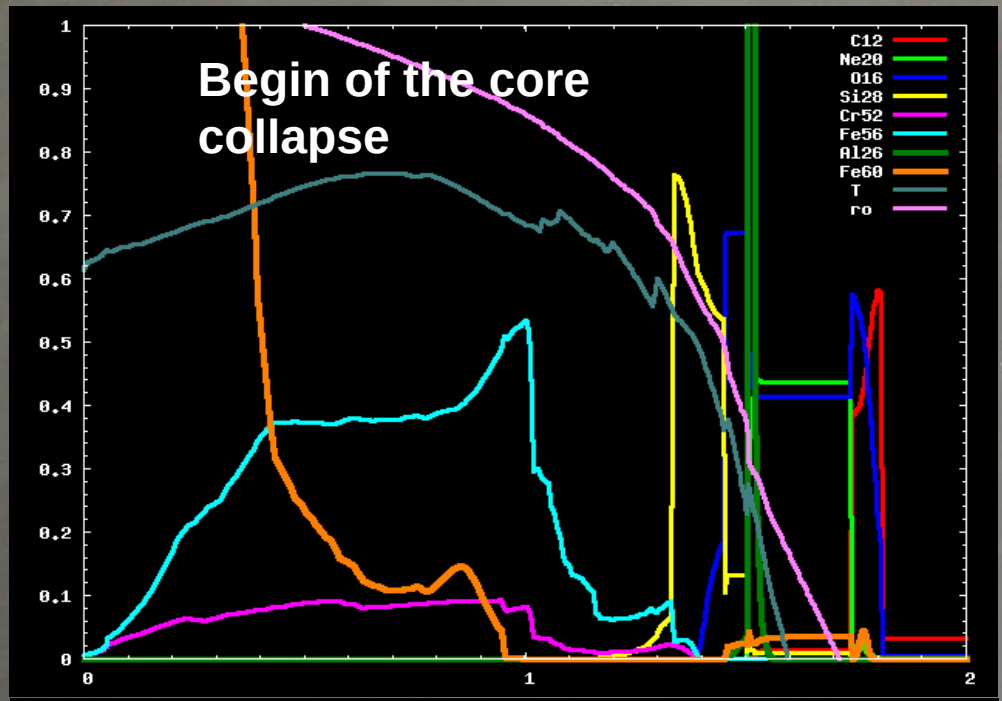
Begin of the core collapse
C12
Ne20
O16
Si28
Cr52
Fe56
Al26
Fe60
T
ro
0
0.1
0.2
0.3
0.4
0.5
0.6
0.7
0.8
0.9
1
0
1
2

120 M_O

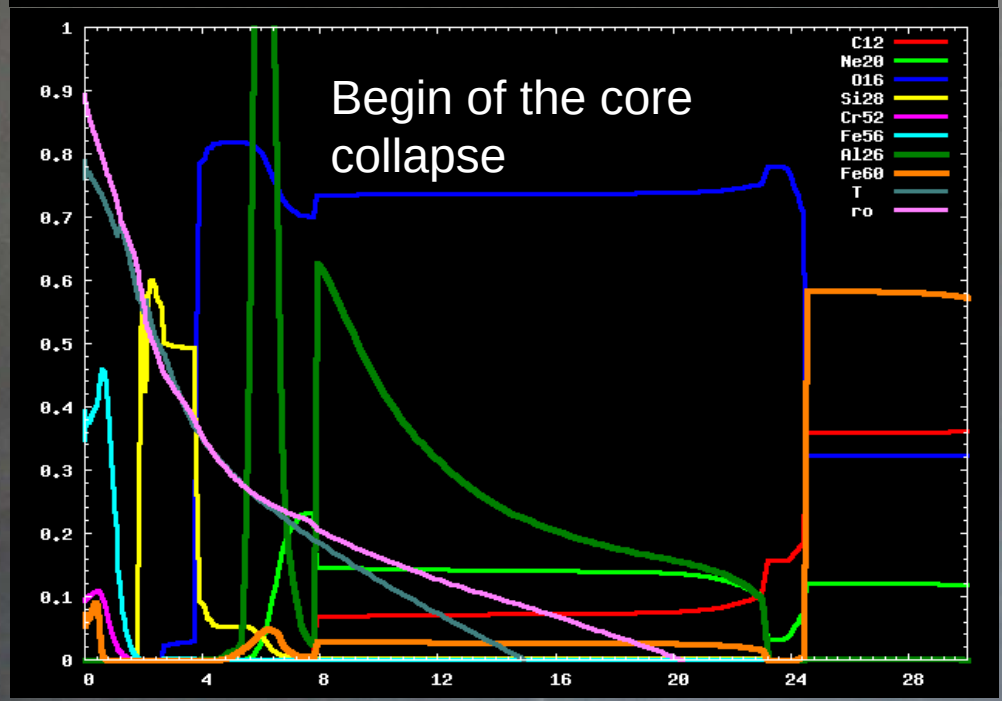
Begin of the core collapse
C12
Ne20
O16
Si28
Cr52
Fe56
Al26
Fe60
T
ro
0
0.1
0.2
0.3
0.4
0.5
0.6
0.7
0.8
0.9
1
0
4
8
12
16
20
24
28

Thank You !

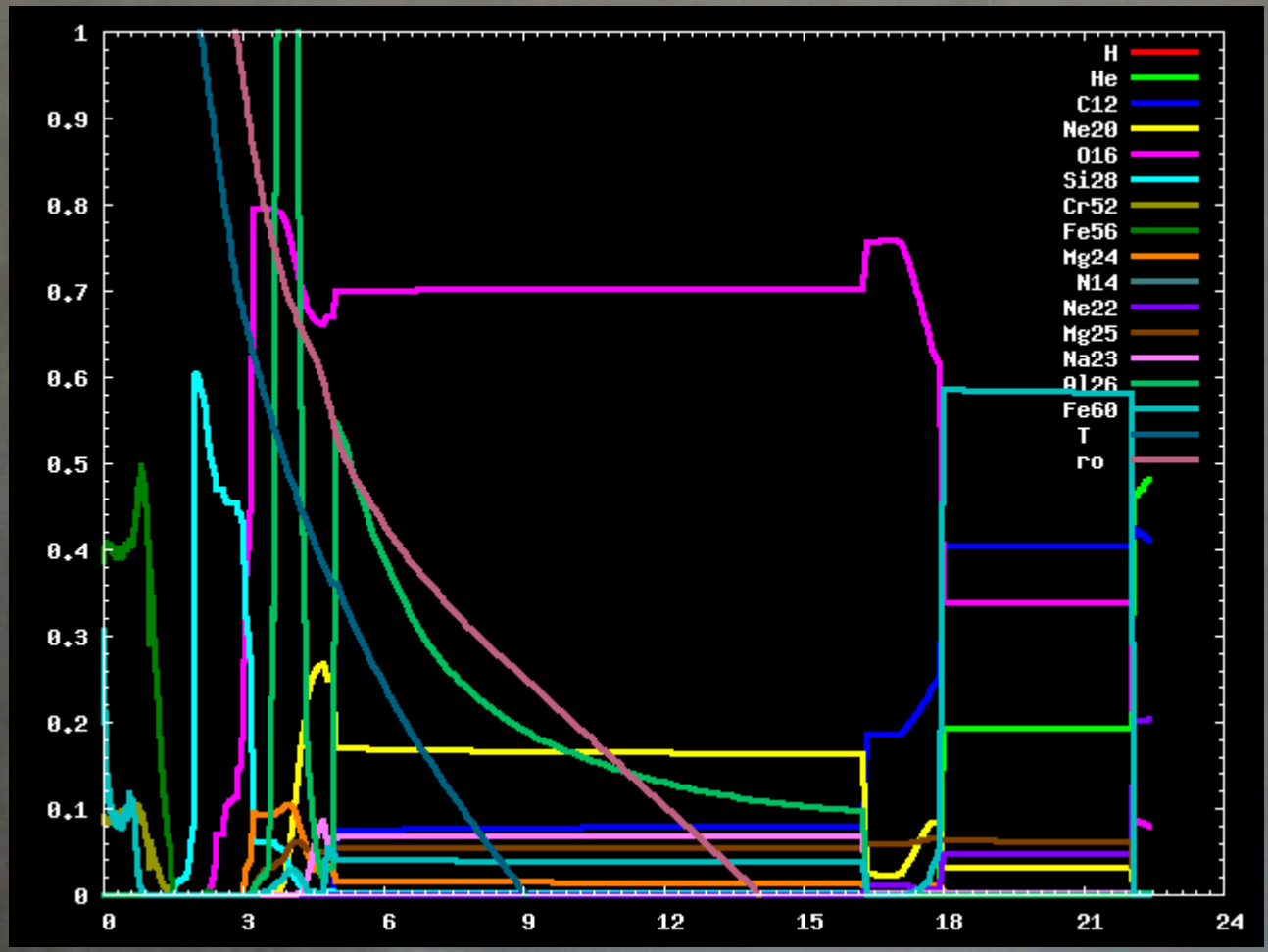
1
0.9
0.8
0.7
0.6
0.5
0.4
0.3
0.2
0.1
0
0
3
6
9
12
15
18
21
24
H
He
C12
Ne20
O16
Si28
Cr52
Fe56
Mg24
N14
Ne22
Mg25
Na23
Al26
Fe60
T
ro

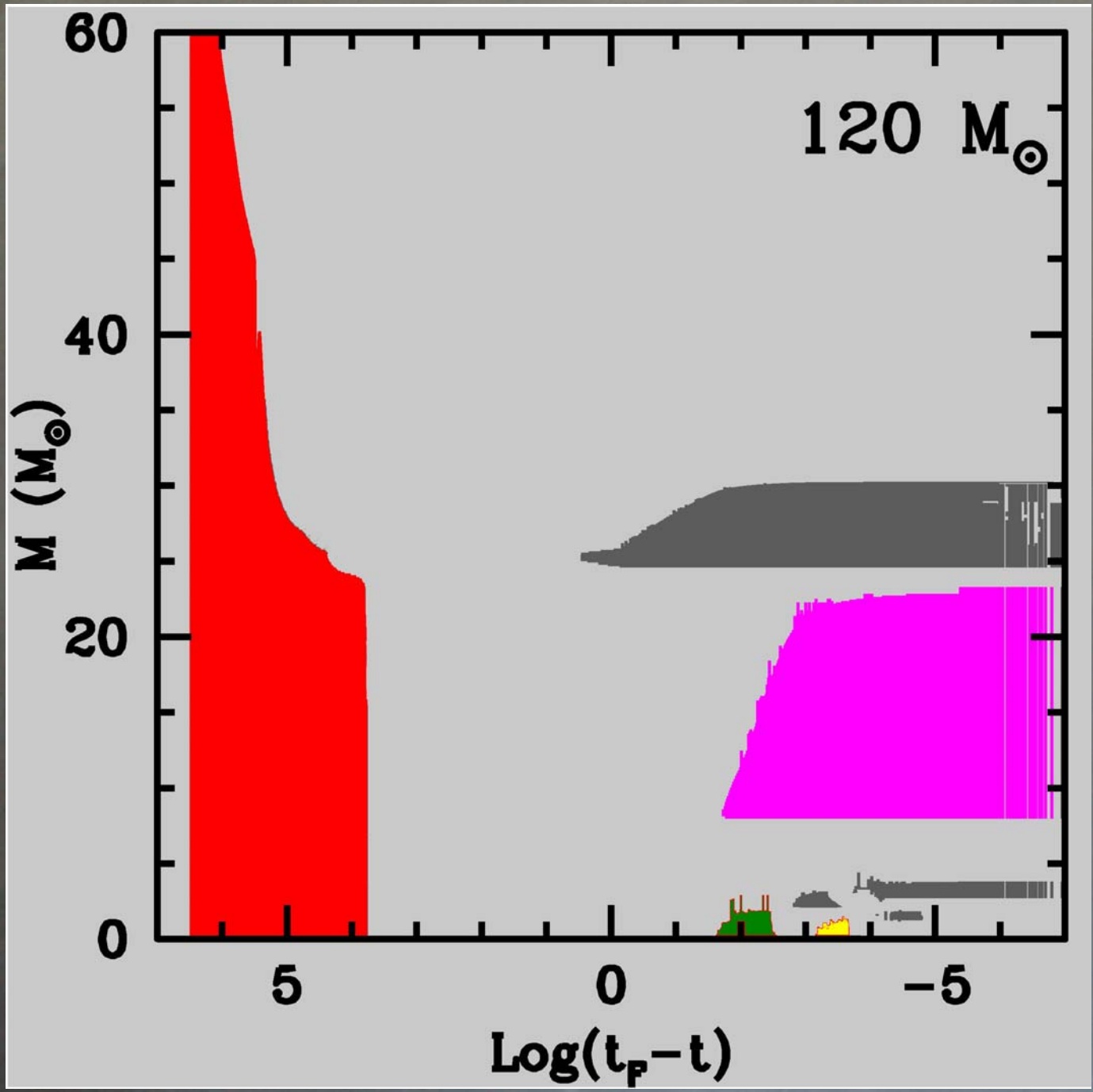
60
40
20
0
M (M⊙)
120 M⊙
5
0
−5
Log(t_F − t)

Basic core collapse scenario

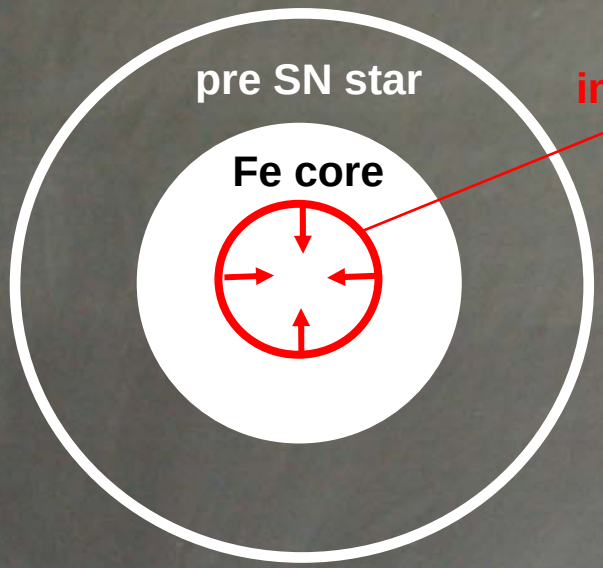

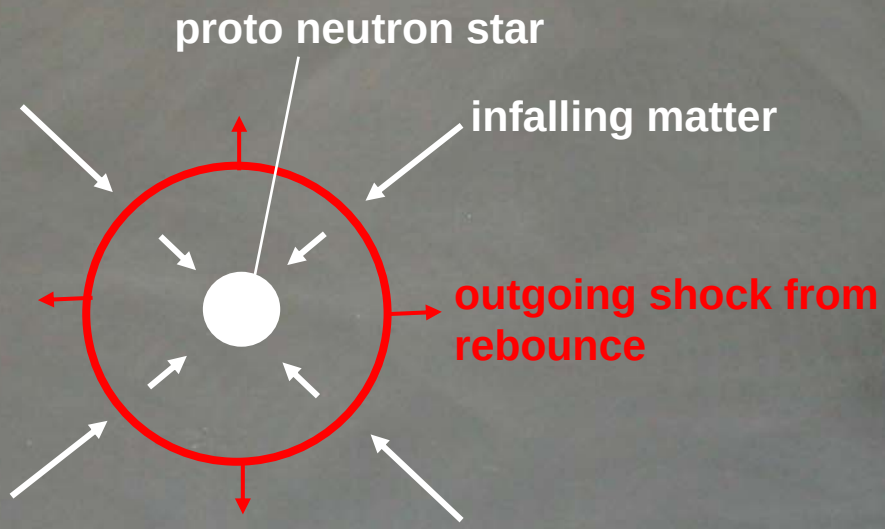

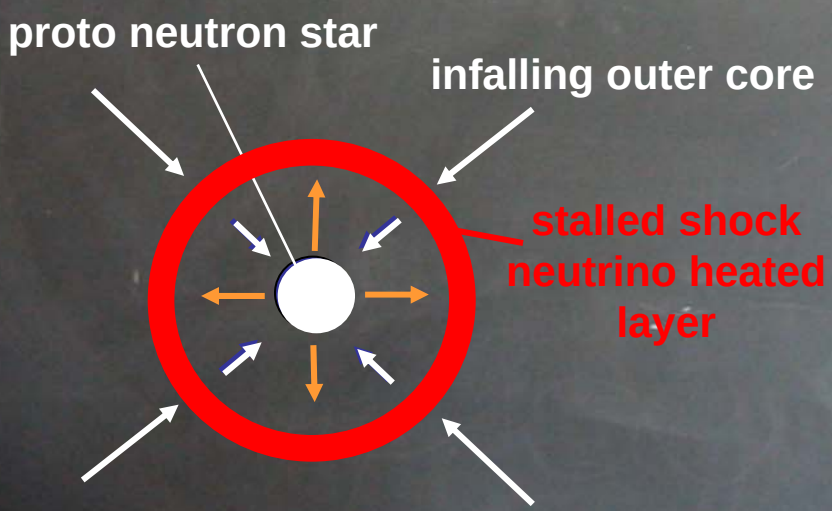

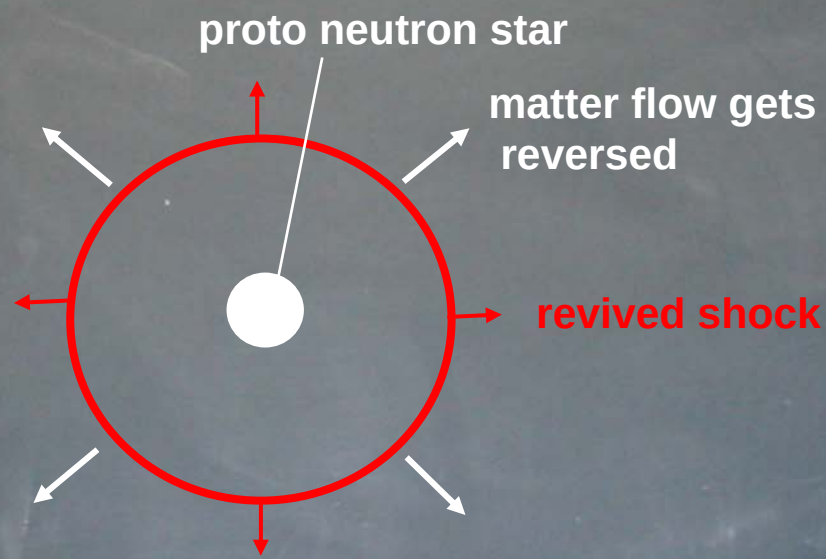

In spite of the many efforts, no successful explosion has been obtained yet

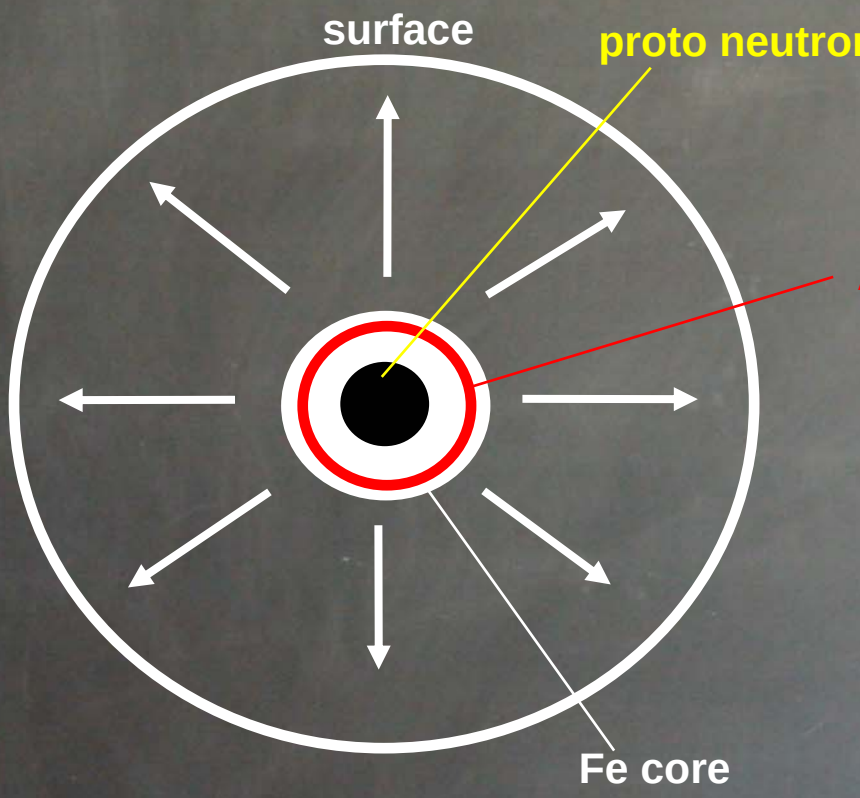

Escamotage:

Assume that a shock wave escapes the Fe core

Since the explosion is not obtained "naturally" a few assumptions are unavoidable:

1) Energy deposited in the shock front

2) Time delay between c.c. and the escape of the shock front from the Fe core

Three different tecniques have been used up to now:

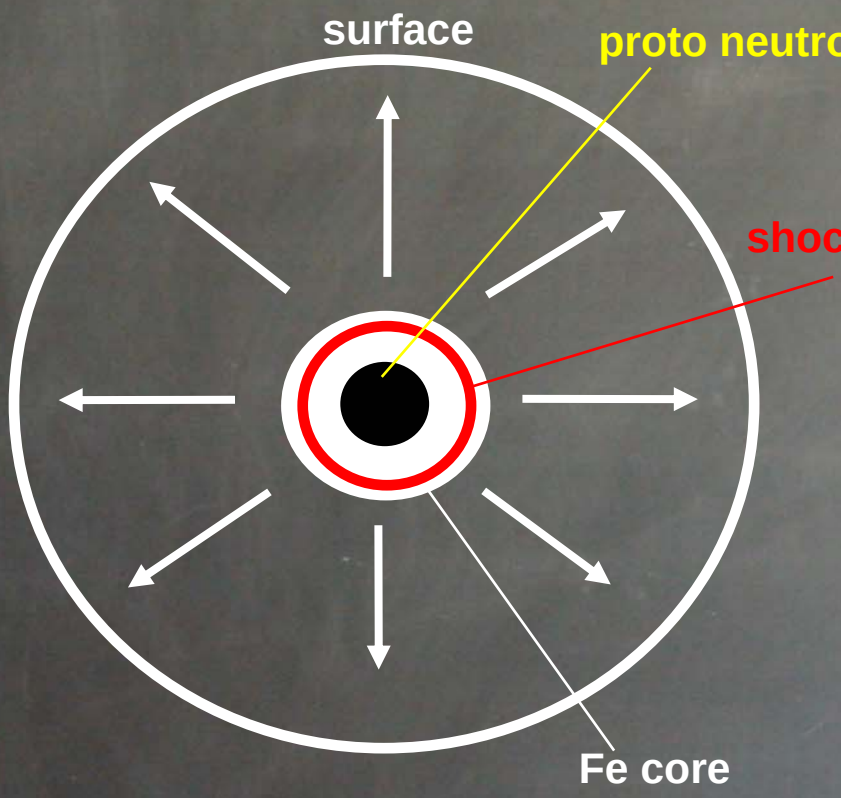

The piston (Woosley and coworkers)

The thermal bomb (Nomoto and coworkers)

The kinetic bomb (Limongi and Chieffi)

"HYDROSTATIC" ELEMENTS

He (^{4}He) $H_{c,s}$ ↑ $He_{c,s}$↓
C (^{12}C) $He_{c,s}$↑ $C_{c,s}$ ↓
N (^{14}N) $H_{c,s}$ ↑ $He_{c,s}$↓
O(^{16}O) He_{c} ↑ Ne_{s} ↑ O_{x}↓
F (^{19}F) He_{s} ↑

- Convection
- $^{12}C(\alpha,\gamma)^{16}O$

"HYDROSTATIC"&"EXPLOSIVE" ELEMENTS

Ne (^{20}Ne) C_{s} ↑ Ne_{x} ↓
Na (^{23}Na) C_{s} ↑ Ne_{x}↓
Mg (^{24}Mg) C_{s}↑ Ne_{x}↓
Al (^{27}Al) C_{s} ↑ Ne_{x}↓
P (^{31}P) Ne_{x}↑
Cl ^{35}Cl(Ne_{x}↑) ^{37}Cl(C_{s}↑ Ne_{x}↓)

- C_{shell} properties
- $^{12}C(\alpha,\gamma)^{16}O$
- Shock wave energy

PURE "EXPLOSIVE" ELEMENTS

Si (^{28}Si) Si_{xi} ↑ O_{x}↑
S (^{32}S) Si_{xi} ↑ O_{x}↑
Ar (^{36}Ar) Si_{xi} ↑ O_{x}↑
Ca (^{40}Ca) Si_{xi} ↑ O_{x}↑
K (^{39}K) O_{x}↑

- M-R relation
- electron density Ye

V (^{51}V) Si_{xi} ↑
Cr (^{52}Fe) Si_{xi} ↑
Mn (^{55}Fe ^{55}Co) Si_{xi} ↑

- Shock wave energy
- Mass cut
- Time delay
- (freeze out)

Sc (^{45}Sc, ^{45}Ca) Si_{x}↑ (C_{s}↑ Ne_{x}↓)
Ti (^{48}Cr) Si_{x} ↑ (Si_{xi} ↑)
Fe (^{56}Ni ^{56}Fe ^{54}Fe) Si_{xi} ↑ Si_{x} ↑
Co (^{59}Ni) Si_{x} ↑
Ni (^{58}Ni) Si_{x} ↑

11 M_O

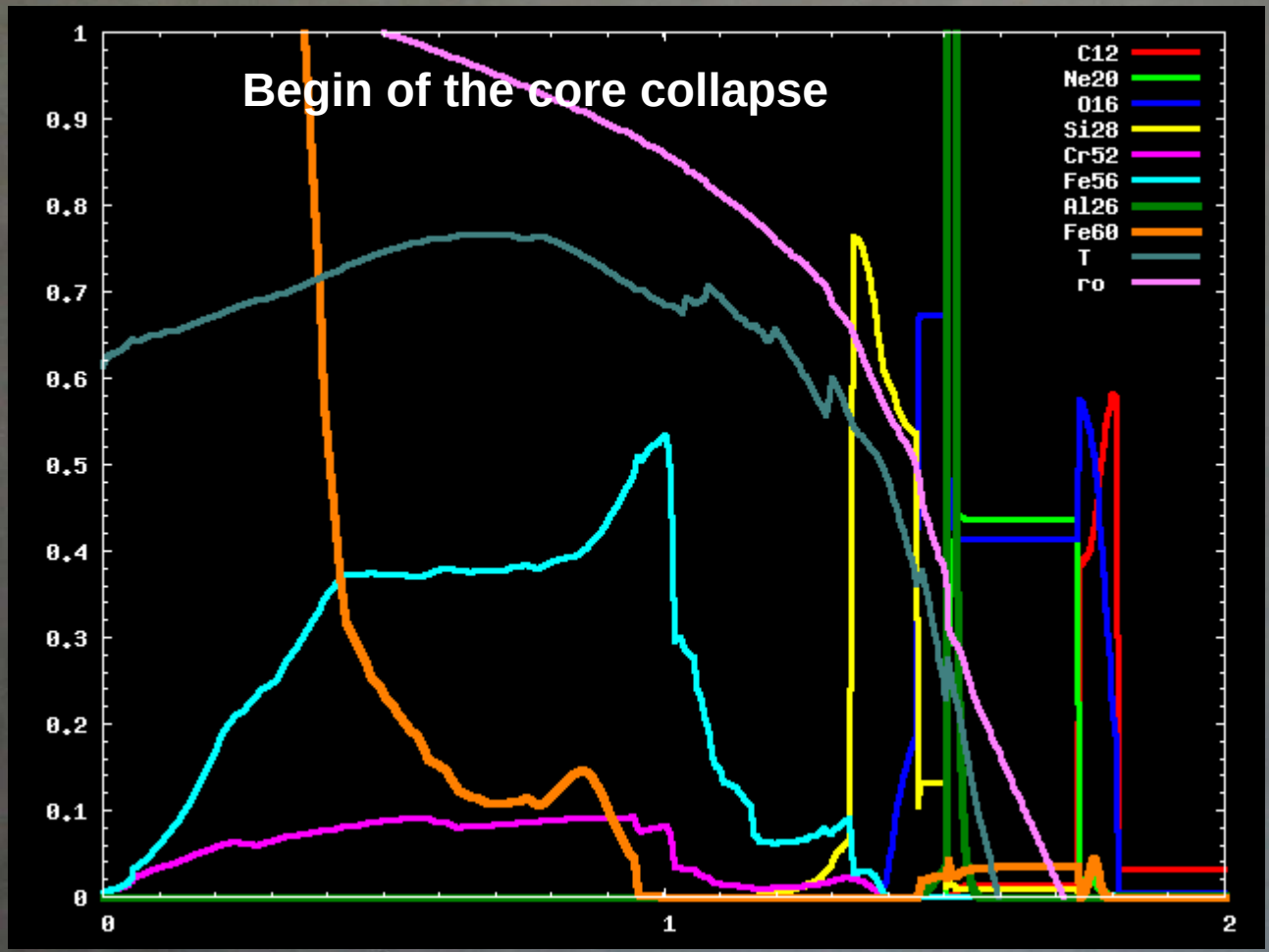
Begin of the core collapse
C12
Ne20
O16
Si28
Cr52
Fe56
Al26
Fe60
T
ro
1
0.9
0.8
0.7
0.6
0.5
0.4
0.3
0.2
0.1
0
0
1
2

120 M_O

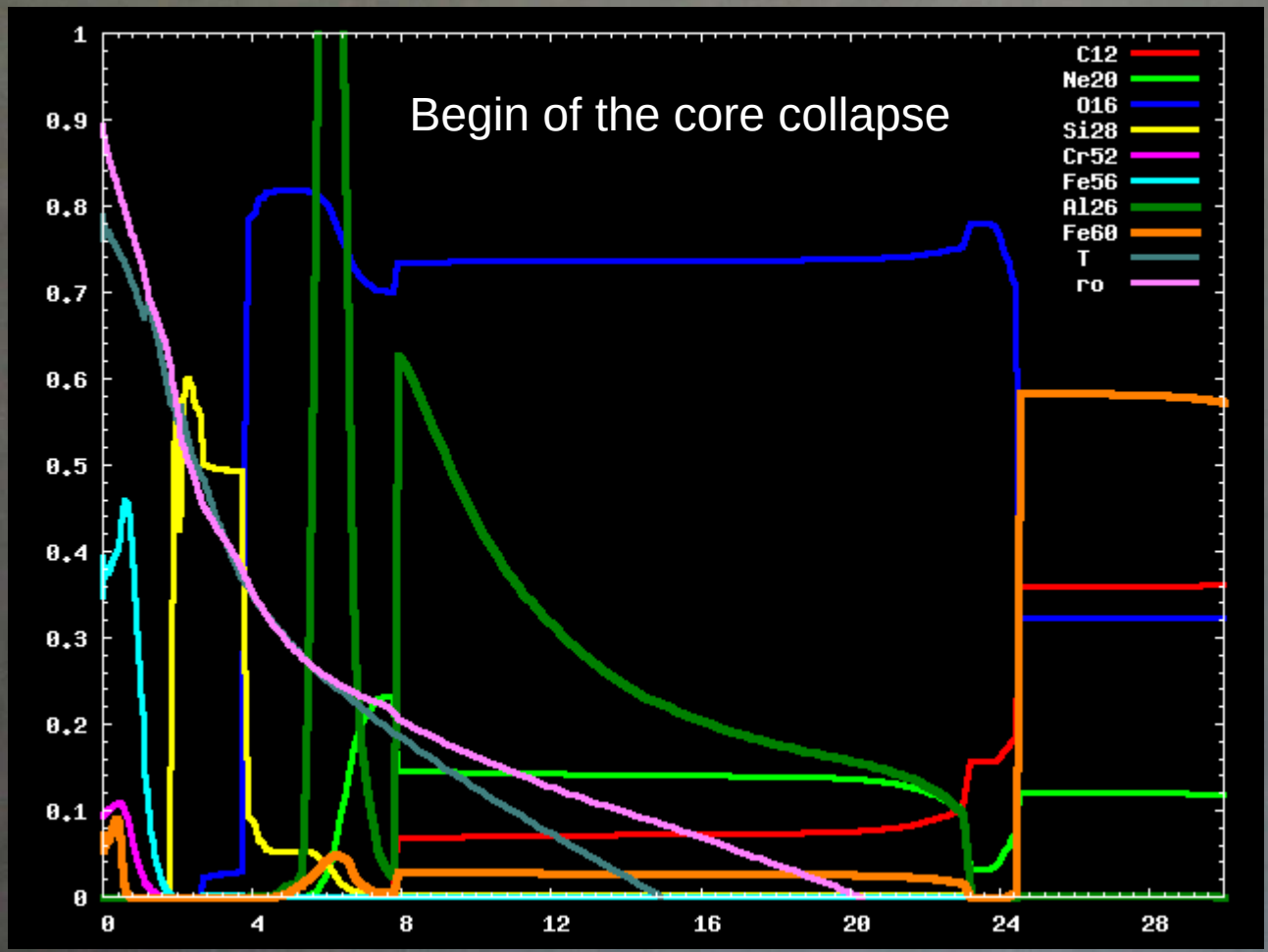
Begin of the core collapse
C12
Ne20
O16
Si28
Cr52
Fe56
Al26
Fe60
T
ro
1
0.9
0.8
0.7
0.6
0.5
0.4
0.3
0.2
0.1
0
0
4
8
12
16
20
24
28